International Journal of Thermophysics, Vol. 8, No. 3, 1987

Thermal Conductivity of Ethane in the Critical Region

P. Desmarest[1] and R. Tufeu[1]

Received June 20, 1986

A coaxial cylinder method was used to measure the thermal conductivity of ethane in the pressure range from 10 up to 280 bar and in the temperature range from 308 up to 365 K.

KEY WORDS: critical region; ethane; high pressure; thermal conductivity.

1. INTRODUCTION

Many measurements of the thermal conductivity of ethane have been reported. An exhaustive bibliography has been published by Prasad and Venart [1]. But only a few authors, Tufeu et al. [2] and Prasad and Venart [1], have covered particularly the critical region. Therefore, new measurements of the thermal conductivity were necessary. In this paper, measurements in the temperature range 308–365 K and at densities up to 1.8 ρ_c are reported. The behavior of the critical thermal conductivity excess along the critical isochore is compared with the theory. An empirical correlation of the thermal conductivity as a function of density and temperature is proposed.

2. EXPERIMENTAL METHOD

The thermal conductivity was measured with a concentric cylinder apparatus previously described in the literature [3, 4]. The experimental procedure was identical to that used, for example, in measuring the thermal conductivity of *n*-butane [5] and propane [6]. The fluid is located in the annular gap between two coaxial cylinders, with the axis in the vertical

[1] Laboratoire des Interactions Moléculaires et des Hautes Pressions–CNRS, Université Paris-Nord, Avenue J. B. Clément, 93430 Villetaneuse, France.

0195-928X/87/0500-0293$05.00/0

direction. The thermal conductivity was determined by measuring the temperature difference between the inner and the outer cylinders as a function of the energy dissipated from the inner cylinder. The temperature difference between the two cylinders varies from 0.3°C close to the critical point to about 2°C far away from the critical point; this temperature difference was measured with an accuracy of approximately 0.003°C. The temperature was measured with an accuracy of 0.02°C, and the pressure with an accuracy of 0.1%.

To determine the thermal conductivity coefficient, we need to consider the correlations due to heat transferred by radiation, spurious heat flow from the inner to the outer cylinder through the solid centering pins and the wires, and heat transferred by convection and the effects of a possible temperature jump at the boundaries of the fluid layer and surfaces of the cylinders [4].

We calculated the radiation correction from the Stefan–Boltzmann radiation law assuming that the absorption of radiation by the fluid could be neglected.

The correction for heat losses through the solid parts of the cell was determined from a set of calibration measurements with argon, neon, and helium, for which the thermal conductivity is known with considerable accuracy [7]. These calibrations were performed at pressures of 1 MPa for argon, 5 MPa for neon, and 10 MPa for helium, i.e., at pressures for which any temperature jump can be neglected [4].

The convection which takes place in the cell is assumed to be laminar. In that case, the correction for convection heat flow Q_c is approximated by the relation [8]

$$Q_c = \mathrm{Ra}\,\frac{2\pi r}{720}\,\lambda\,\Delta T \tag{1}$$

where Ra is the Rayleigh number, λ is the thermal conductivity of the fluid, r is the radius of the inner cylinder, and ΔT is the temperature difference between the cylinders.

3. RESULTS

The thermal conductivity of ethane was measured along six quasi-isotherms: 308, 311, 315, 322, 335, and 364 K. The experimental data are presented in Table AI in the Appendix. We have represented in Fig. 1 the experimental data as a function of the density along quasi-isotherms. The densities ρ were calculated from an equation of state developed at the

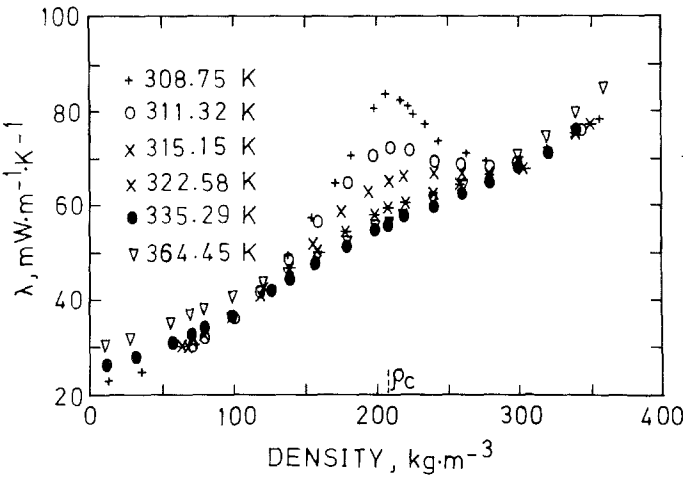

Fig. 1. The thrmal conductivity of ethane as a function of density and temperature.

National Bureau Standard (Boulder). The critical parameters are the following:

$$T_c = 305.33 \text{ K}; \qquad P_c = 4.872 \text{ MPa}; \qquad \rho_c = 206.5 \text{ kg} \cdot \text{m}^{-3}$$

4. DATA ANALYSIS

Following the decomposition suggested by Sengers et al. [9], the thermal conductivity was written as

$$\lambda(\rho, T) = \lambda_B(\rho, T) + \Delta\lambda_c(\rho, T) \tag{2}$$

where $\lambda_B(\rho, T)$ is the background thermal conductivity, which is defined by

$$\lambda_B(\rho, T) = \lambda_0(T) + \Delta\lambda(\rho) \tag{3}$$

$\lambda_0(T)$ is the zero-density thermal conductivity, $\Delta\lambda(\rho)$ is the normal density effect, and $\Delta\lambda_c(\rho, T)$ is the critical enhancement of the thermal conductivity.

4.1. The Background Thermal Conductivity

$\lambda_0(T)$ was obtained by extrapolation, at each temperature of the data obtained at low density. $\lambda_0(T)$ can be represented, for the restricted temperature range 300–370 K, by a linear temperature dependence:

$$\lambda_0(T) = a + bT \tag{4}$$

with

$$a = -19.774, \qquad b = 0.136$$

T is in K and $\lambda_0(T)$ is in $\mathrm{mW \cdot m^{-1} \cdot K^{-1}}$.

In the temperature range considered, we can assume that $\Delta\lambda(\rho)$ is a function of density alone. Therefore, the normal density effect has been deduced from the behavior of the thermal conductivity far away from the critical point. The data of Tufeu et al. [2], Le Neindre et al. [10], and Prasad and Venart [1], in the temperature range $T \geqslant 500$ K, were used for this determination. The normal density effect has been fitted to a power series in density and can be written as

$$\Delta\lambda(\rho) = \sum_{j=1}^{4} B_j \rho^j \tag{5}$$

with

$$B_1 = 5.9223, \qquad E-02$$
$$B_2 = 2.84339, \qquad E-04$$
$$B_3 = -9.56254, \qquad E-07$$
$$B_4 = 2.43563, \qquad E-09$$

ρ is in $\mathrm{kg \cdot m^{-3}}$ and $\Delta\lambda$ is in $\mathrm{mW \cdot m^{-1} \cdot K^{-1}}$.

4.2. Theoretical Representation of the Critical Enhancement

The critical enhancement $\Delta_{\lambda_c}(\rho, T)$ was estimated by subtracting the background thermal conductivity $\lambda_B(\rho, T)$ [Eqs. (3)–(5)] from the experimental data of the thermal conductivity. We can see that the mximum of $\Delta\lambda_c(\rho, T)$ occurs at ρ_c as shown in Fig. 2.

Our values of $\Delta\lambda_c(\rho_c, T)$ are in good agreement with those of Tufeu et al. [2] but the values obtained by Prasad and Venart [1] are 20% larger. The transient hot-wire method used in Ref. 1 is not an accurate technique of measurement for the critical thermal conductivity excess close to the critical point.

The critical thermal conductivity excess along the critical isochore can be written as [11]

$$\Delta\lambda_c(\rho_c, T) = A \frac{k_B T}{6\pi\eta\xi} \rho_c C_p^c F(t) \tag{6}$$

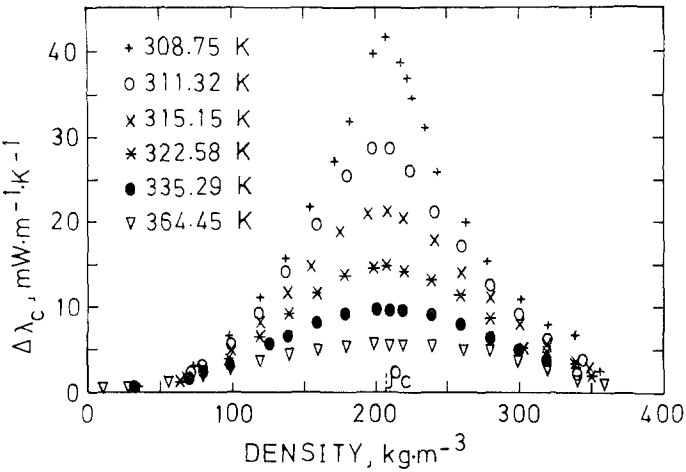

Fig. 2. The ethane thermal conductivity critical enhancement.

where $t=(T-T_c)/T_c$, η is the shear viscosity estimated from the data of Diller and Saber [12],

$$C_p^c = C_p - C_v = \frac{T}{\rho_c}\left(\frac{dP}{dT}\right)^2_{\rho_c} K_T$$

and K_T is the isothermal compressibility proposed by Garrabos [13].

In the temperature range $t<0.02$, K_T was written as

$$K_T = K_T^0 t^{-\gamma}[1 + a_x t^{\Delta}] \tag{7}$$

with

$$K_T^0 = 1.069 \times 10^{-8}\ \text{Pa}^{-1}, \qquad a_x = 1.638$$
$$\gamma = 1.24 \qquad\qquad \Delta = 0.5$$

In the temperature range $0.02<t<0.1$, K_T was calculated by an empirical correlation:

$$K_T = 1.6986\, t^{-1.16665} \times 10^{-8}\ \text{Pa}^{-1} \tag{8}$$

The correlation length ξ along the critical isochore is represented by

$$\xi = \xi_0 t^{-\nu}[1 + a_\xi t^{\Delta}] \tag{9}$$

with

$$\xi_0 = 1.7946 \times 10^{-10}\ \text{m}, \qquad a_\xi = 1.0534$$

$$\nu = 0.63$$

Another determination of K_T and ξ has been proposed by Sengers and Sengers [14]. The isothermal compressibility was represented by

$$K_T = 1.4388\, t^{-\gamma} \times 10^{-8}\ \text{Pa}^{-1} \tag{10}$$

with $\gamma = 1.19$.

The correlation length was calculated by the following expression:

$$\xi = 1.8\, t^{-\nu} \times 10^{-10}\ \text{m}$$

with $\nu = 0.633$.

Table I shows the values of the critical enhancement of the thermal conductivity along the critical isochore calculated with the values of K_T and ξ obtained by the equation of Garrabos and Sengers, by setting $\Lambda = 1.2$. $F(t) = e^{-At}$ is an exponential damping function, where $A = 18.6$ is an adjustable constant [11].

We can see that the experimental data of $\Delta\lambda_c(\rho_c, T)$ are in a reasonable agreement with these two data sets.

Figure 3 shows $\Delta\lambda_c(\rho_c, T)$ as a function of ΔT in a logarithmic scale.

5. EMPIRICAL CORRELATION FOR THE THERMAL CONDUCTIVITY OF ETHANE

Following the method used for NH_3 [15], an empirical correlation is proposed. Our determination of $\lambda(\rho, T)$ is based on Eq. (2), where λ_B is given by Eqs. (3)–(5).

Table I. Critical Enhancement of the Thermal Conductivity of Ethane Along the Critical Isochore Calculated from Eq. (6)

$T - T_c$ (K)	$\Delta\lambda_c(\rho_c, T)$ cal. (mW · m^{-1} · K^{-1})		$\Delta\lambda_c(\rho_c, T)$ exp. (mW · m^{-1} · K^{-1})
	Ref. 13	Ref. 14	
3.42	39.70	39.79	41.6
5.99	28.15	29.55	28.8
9.82	21.24	22.88	21.1
17.82	15.25	—	14.7
29.96	10.19	—	9.7

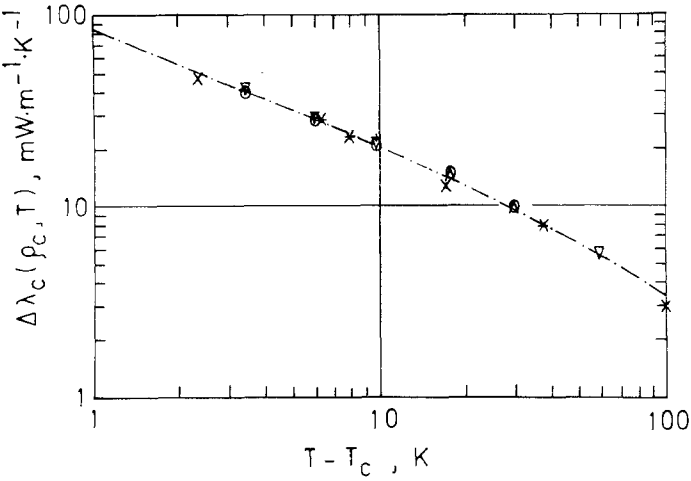

Fig. 3. The critical enhancement of the thermal conductivity of ethane for the critical density as a function of the temperature difference $(T - T_c)$. (∇) Present data; ($*$) data from Ref. 2; ($\square$) calculated Eq. (6), K_T and ξ from Ref. 13; ($+$) calculated Eq. (6), K_T and ξ from Ref. 14; (——) calculated Eq. (13).

For $\rho > \rho_c$ our data can be represented by

$$\Delta\lambda_c(\rho, T) = \Delta\lambda_c(\rho_c, T)\frac{X(T)^2}{X(T)^2 + (\rho - \rho_c)^2} \tag{11}$$

The width $X(T)$ of the Lorentzian is fitted by

$$X(T) = 0.617\,\rho_c + 16.0625 \ln t \tag{12}$$

$\Delta\lambda_c(\rho_c, T)$ is the maximum of the critical enhancement represented by

$$\Delta\lambda_c(\rho_c, T) = At^{-0.57}(1 + Bt^{0.5} + Ct) \tag{13}$$

with

$$A = 3.44125\ \text{mW} \cdot \text{m}^{-1} \cdot \text{K}^{-1}$$

$$B = -0.7483$$

$$C = -0.14429$$

In the density range $\rho < \rho_c$, the critical enhancement is written

$$\Delta\lambda_c(\rho, T) = \Delta\lambda_c(\rho_c, T) \frac{X'(T)^2}{X'(T)^2 + (\rho_c - \rho)^2} \exp\left[-5\left(\frac{\rho}{\rho_c} - 1\right)^4\right] \quad (14)$$

with

$$X'(T) = 0.630\,\rho_c + 16.0625 \ln t \quad (15)$$

and $\Delta\lambda_c(\rho_c, T)$ is calculated by Eq. (13).

A comparison between the experimental data and the values obtained by the correlation is reported in Fig. 4. The experimental data are within 2% of those estimated by the correlation, but for the 308.75 K isotherm, the deviation reaches 5%. This deviation can be explained by an error on the density coming from the equation of state or by an error on P and T or by the function form chosen to represent $\Delta\lambda_c$.

6. CONCLUSION

Measurements of thermal conductivity are now available for several hydrocarbons such as as *n*-butane, isobutane, propane, and ethane, particularly in the critical region. A comparative study of the critical thermal conductivity excess of these hydrocarbons will be presented in a forthcoming paper.

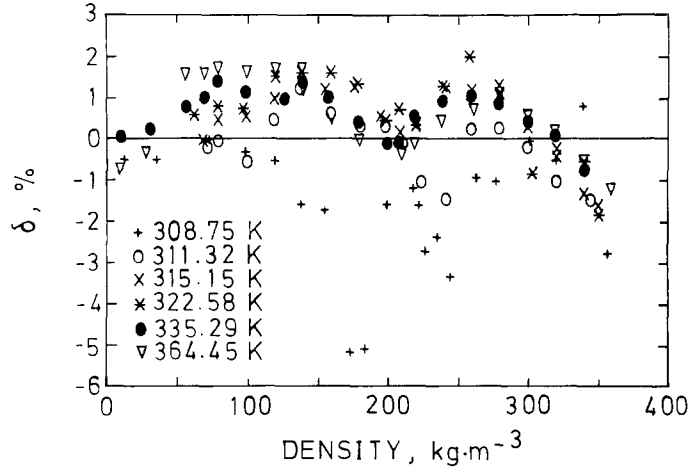

Fig. 4. Deviation of experimental data from the proposed correlation [Eqs. (2)–(5) and (11)–(14)].

APPENDIX

Table AI. Experimental Data of the Thermal Conductivity of Ethane and Comparison with the Proposed Correlation

T (K)	P (MPa)	ρ (kg·m^{-3})	λ (mW·m^{-1}·K^{-1})	δ (%)
308.39	9.576	357.0	78.21	−2.85
308.45	7.974	340.0	76.76	0.75
308.53	6.728	320.2	72.01	−0.54
308.59	6.030	301.5	70.17	−0.10
308.63	5.573	278.3	69.30	−1.07
308.63	5.424	264.0	71.03	−1.00
308.75	5.330	244.6	73.60	−3.37
308.69	5.290	235.7	77.31	−2.41
308.73	5.270	227.0	79.43	−2.75
308.73	5.260	223.0	81.30	−1.67
308.75	5.250	218.7	82.33	−1.23
308.75	5.230	208.2	83.77	0.07
308.75	5.213	200.0	80.74	−1.65
308.82	5.188	183.5	70.69	−5.12
308.87	5.167	172.8	64.63	−5.19
308.99	5.127	155.8	57.35	−1.76
309.01	5.046	138.5	49.36	−1.62
309.05	4.904	120.3	42.85	−0.55
309.17	4.620	98.91	36.32	−0.34
309.19	4.042	73.77	30.60	−0.05
308.75	2.492	36.09	24.97	−0.51
308.80	0.9980	12.54	22.96	−0.50
311.33	9.281	345.0	76.00	−1.54
311.31	7.386	320.4	71.15	−1.07
311.35	6.535	300.0	68.91	−0.25
311.36	6.059	280.0	68.04	0.20
311.35	5.796	260.3	68.63	0.19
311.33	5.654	242.1	69.37	−1.50
311.30	5.562	224.5	71.60	−1.07
311.32	5.512	211.2	72.22	−0.12
311.34	5.471	198.9	70.50	0.24
311.34	5.410	181.1	64.92	0.28
311.38	5.329	159.9	56.47	0.59
311.42	5.208	138.8	48.59	1.20
311.45	5.025	119.1	41.78	0.43
311.51	4.752	100.5	36.25	−0.59
311.57	4.296	80.13	31.87	−0.04
311.58	4.053	71.85	30.26	−0.22
315.19	10.900	350.1	77.15	−1.68
315.15	9.858	340.5	74.92	−1.35

Table AI. *(Continued)*

T (K)	P (MPa)	ρ (kg·m^{-3})	λ (mW·m^{-1}·K^{-1})	δ (%)
315.15	8.288	320.4	71.16	−0.47
315.15	7.315	300.6	68.44	0.22
315.17	6.717	280.3	67.11	1.25
315.15	6.363	260.7	66.36	1.16
315.16	6.150	241.6	66.60	1.22
315.19	5.988	220.3	65.86	0.27
315.15	5.917	209.8	64.99	0.14
315.17	5.836	195.5	62.83	0.52
315.22	5.734	176.7	58.28	1.23
315.24	5.603	155.9	51.78	1.17
315.28	5.471	139.5	46.95	1.57
315.35	5.258	120.5	41.36	0.96
315.38	4.904	99.60	36.11	0.52
513.44	4.417	79.89	32.09	0.45
315.48	4.053	68.58	30.01	−0.05
322.51	13.172	350.6	77.38	−1.89
322.51	11.814	339.7	75.42	−0.60
322.52	10.061	320.8	71.23	−0.26
322.53	8.970	303.8	67.59	−0.88
322.54	7.984	279.9	65.57	1.07
322.54	7.437	259.1	64.25	1.92
322.58	7.102	240.0	62.64	1.25
322.55	6.839	220.7	60.73	0.35
322.58	6.707	208.5	59.56	0.68
322.58	6.606	199.3	58.02	0.41
322.61	6.404	179.0	54.52	1.30
322.63	6.201	159.4	50.06	1.58
322.56	5.957	139.4	45.30	1.70
322.71	5.653	119.9	40.72	1.48
322.73	5.187	98.22	35.95	0.72
322.79	4.650	79.71	32.67	0.79
322.82	4.053	63.72	30.20	0.58
335.23	15.533	341.0	76.49	−0.80
335.23	13.010	319.6	71.84	0.09
335.25	11.389	299.9	68.03	0.40
335.28	10.243	280.2	65.08	0.83
335.28	9.402	260.0	62.60	1.04
335.29	8.784	239.8	60.31	0.86
335.28	8.308	219.9	57.94	0.52
335.29	8.095	209.6	56.27	−0.10
335.31	7.923	200.6	54.97	−0.13
335.33	7.548	179.9	51.81	0.34
335.34	7.174	159.2	48.25	0.99

Table AI. *(Continued)*

T (K)	P (MPa)	ρ (kg·m^{-3})	λ (mW·m^{-1}·K^{-1})	δ (%)
335.37	6.788	139.5	44.60	1.35
335.38	6.515	127.2	42.08	0.95
335.41	5.755	99.45	37.15	1.11
335.43	5.056	79.80	34.12	1.36
335.47	4.640	69.87	32.60	0.99
335.51	4.053	57.54	30.99	0.78
335.22	2.523	31.68	28.18	0.23
335.25	0.993	11.28	26.57	0.05
364.44	28.190	359.9	84.84	−1.29
364.49	23.831	340.8	79.59	−0.56
364.49	20.140	319.9	74.62	0.09
364.49	17.570	300.1	70.50	0.53
364.49	15.563	280.2	67.05	1.00
364.45	14.115	261.9	63.85	0.67
364.49	12.766	240.0	60.57	0.38
364.49	11.753	219.7	57.52	−0.17
364.49	11.328	210.1	56.05	−0.44
364.51	10.912	199.9	54.83	−0.08
364.54	10.162	180.4	51.96	−0.07
364.53	9.423	160.3	49.16	0.47
364.57	8.663	139.9	46.28	1.14
364.58	7.893	120.6	43.52	1.66
364.59	6.981	100.0	40.42	1.58
364.62	5.968	79.92	37.70	1.67
364.65	5.410	69.93	36.43	1.55
364,67	4.569	56.19	34.88	1.55
364.72	2.533	27.99	31.66	−0.36
364.77	1.003	10.35	30.27	−0.74

REFERENCES

1. R. C. Prasad and J. E. S. Venart, *Int. J. Thermophys.* **5**:367 (1984).
2. R. Tufeu, Y. Garrabos, and B. Le Neindre, in *Proc. 16th Int. Conf. Therm. Conduct.*, D. C. Larsen, ed. (Plenum, New York, 1983), p. 605.
3. B. Le Neindre, Thesis (Université Paris VI, Paris, 1969).
4. R. Tufeu, Thesis (Université Paris VI, Paris, 1971).
5. C. A. Nieto de Castro, R. Tufeu, and B. Le Neindre, *Int. J. Thermophys.* **4**:11 (1983).
6. R. Tufeu and B. Le Neindre, *Int. J. Thermophys.* **8**:27 (1987).
7. J. Kestin, R. Paul, A. A. Clifford, and W. A. Wakeman, *Physica* **100A**:349 (1980).
8. P. Johannin, Thesis (Université Paris, Paris, 1958).
9. J. V. Sengers, R. S. Basu, and M. H. Levelt-Sengers, Representative equations for the thermodynamic and transport properties of fluids near the gas-liquid critical point, NASA Contractor Report 3424 (May 1981), p. 59.

10. B. Le Neindre, R. Tufeu, P. Bury, P. Johannin, and B. Vodar, in *Proc. 8th Int. Conf. Therm. Conduct.*, C. Y. Ho and R. E. Taylor, eds. (Plenum, New York, 1969), p. 229.
11. H. J. M. Hanley, J. V. Sengers, and J. F. Ely, in *Proc. 14th Int. Conf. Therm. Conduct.*, P. G. Klemens and T. K. Chu, eds. (Plenum, New York, 1976), p. 383.
12. D. E. Diller and J. M. Saber, *Physica* **108A**:143 (1981).
13. Y. Garrabos, *J. Phys.* **47**:197 (1986).
14. J. V. Sengers and J. M. H. Sengers, in *Progress in Liquid Physics*, C. A. Croxton, ed. (Wiley, New York, 1978), p. 89.
15. R. Tufeu, D. Y. Ivanov, Y. Garrabos, and B. Le Neindre, *Ber. Bunsenges. Phys. Chem.* **88**:422 (1984).